Science Translational Medicine
AAAS

stm.sciencemag.org/cgi/content/full/13/582/eabd6299/DC1

Supplementary Materials for

Mechanism and reversal of drug-induced nephrotoxicity on a chip

Aaron Cohen, Konstantinos Ioannidis, Avner Ehrlich, Shaun Regenbaum, Merav Cohen, Muneef Ayyash, Sigal Shafran Tikva, Yaakov Nahmias*

*Corresponding author. Email: ynahmias@cs.huji.ac.il

Published 24 February 2021, *Sci. Transl. Med.* **13**, eabd6299 (2021)
DOI: 10.1126/scitranslmed.abd6299

The PDF file includes:

Fig. S1. Inhibition of P-gp retains calcein AM in proximal tubule cysts.
Fig. S2. Design and sensitivity of in-line metabolic sensors.
Fig. S3. CsA induces a shift to lipogenesis.
Fig. S4. Cisplatin induces a shift to lipogenesis.
Fig. S5. Glucose inhibition shifts the onset of cellular damage.
Fig. S6. Clinical validation in human patients segmented by sex.
Fig. S7. Expression of endoplasmic reticulum stress markers after drug exposure.
Table S1. Expression analysis of vascularized kidney spheroids.
Table S2. List of qRT-PCR primers.
Table S3. List of antibodies and probes.
Legend for data file S1
Legend for movie S1

Other Supplementary Material for this manuscript includes the following:

(available at stm.sciencemag.org/cgi/content/full/13/582/eabd6299/DC1)

Data file S1 (Microsoft Excel format). Raw data.
Movie S1 (.avi format). 3D reconstruction from LSM700 confocal Z-stack of a vascularized kidney spheroid labeled with AQP1.

Supplementary Information

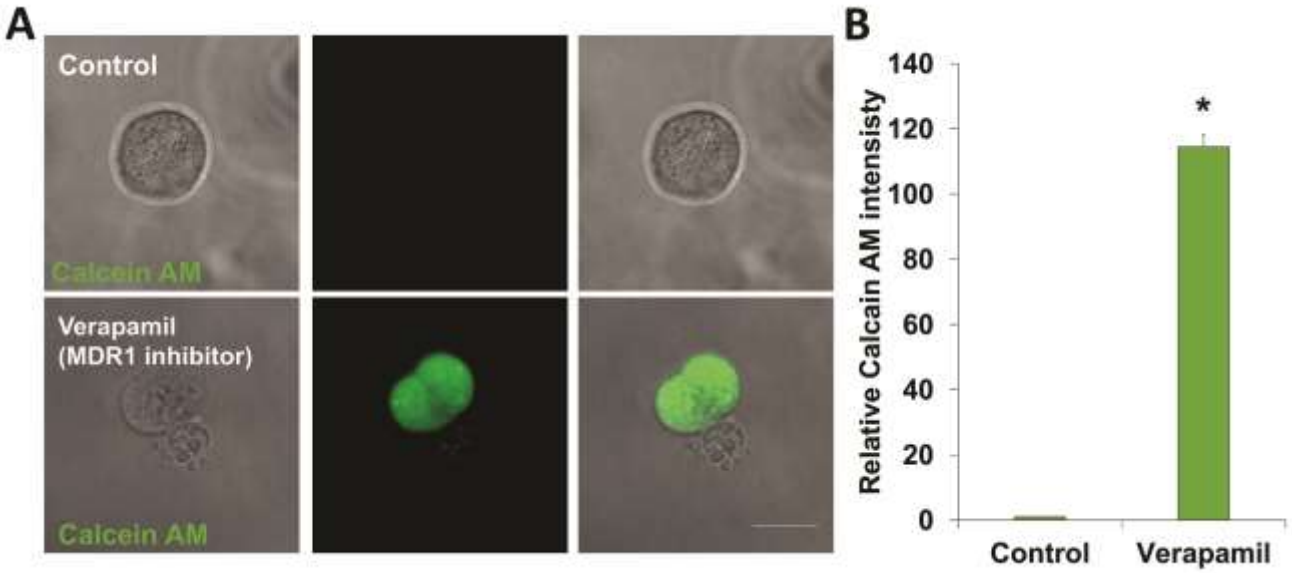

Fig. S1. Inhibition of P-gp retains calcein AM in proximal tubule cysts. (A) Functional polarity assay in cysts exposed to verapamil (100 μM), specific inhibitor of P-gp, for 24 hours. Fluorescent calcein is excreted through MDR1 (P-gp) in polarized cells (control, untreated cysts) but accumulates in cells treated with Verapamil. **(B)** Quantification of calcein accumulation. Student's *t*-test. $*P < 0.05$. Scale bar: 25 μm. n=4. N=3. Error bars indicate ± S.E.

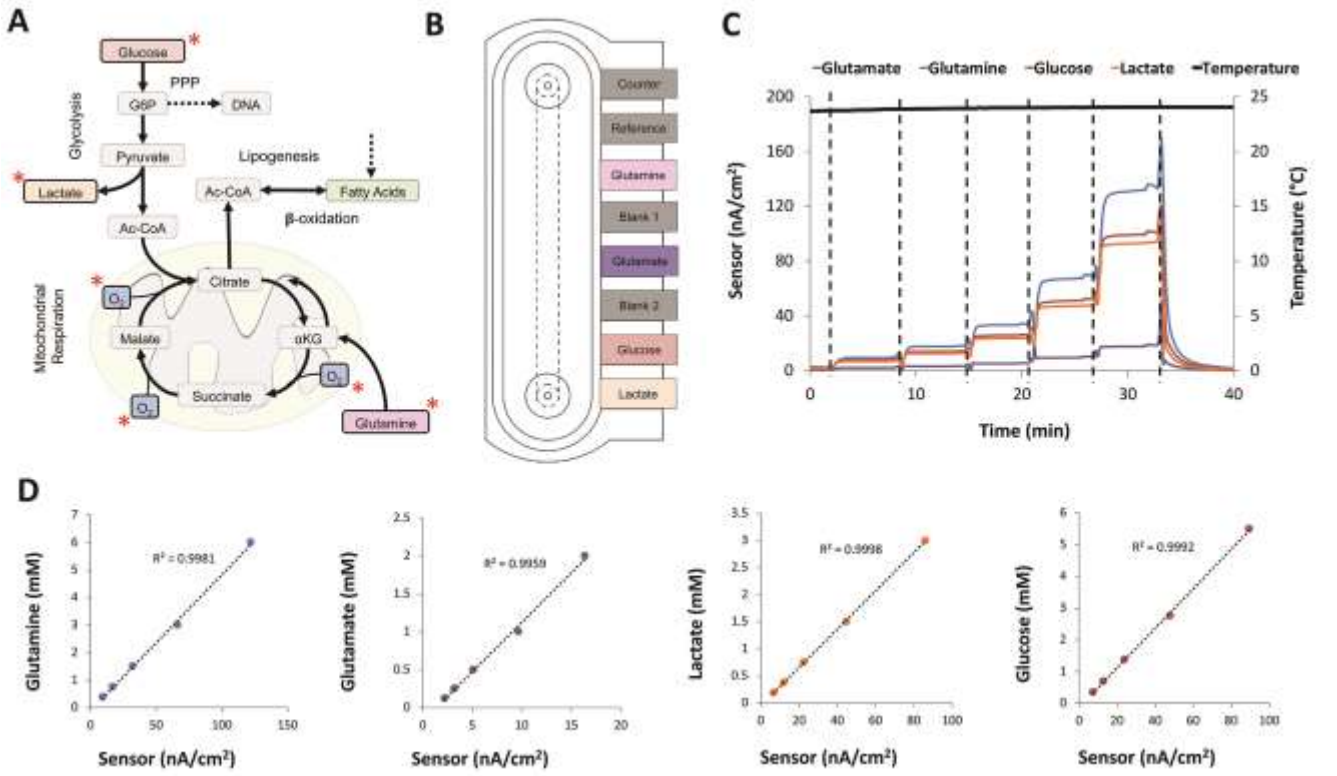

Fig. S2. Design and sensitivity of in-line metabolic sensors. (A) Schematic of central carbon metabolism in human proximal tubule cells. Flux balance analysis permits the calculation of intracellular fluxes (black arrows) using extracellular measurements of oxygen, glucose, lactate, glutamine and glutamate (red stars). Dotted arrows note experimentally limited fluxes. **(B)** Low volume microfluidic amperometric, 8-electrode, 4-analytes biosensor array. Anodic oxidation of H_2O_2 on platinum produces a current rapidly (t_{90} < 25 sec), while embedded catalase activity prevents cross-contamination. A 450-mV potential between the working and counter electrodes is monitored against a reference electrode to minimize background noise caused by reversible electrolysis events. **(C)** Raw measurements of glucose, lactate, glutamine, glutamate and temperature sensors of calibration measurements for different analyte concentrations. Measurements were carried automatically out under continuous flow of 5 µL/min. Air gap between samples ensure a sharp change in chemical gradient on the sensor during in calibration. **(D)** Amperometric calibration curves of glucose, lactate, glutamine and glutamate concentrations in bioreactor outflow.

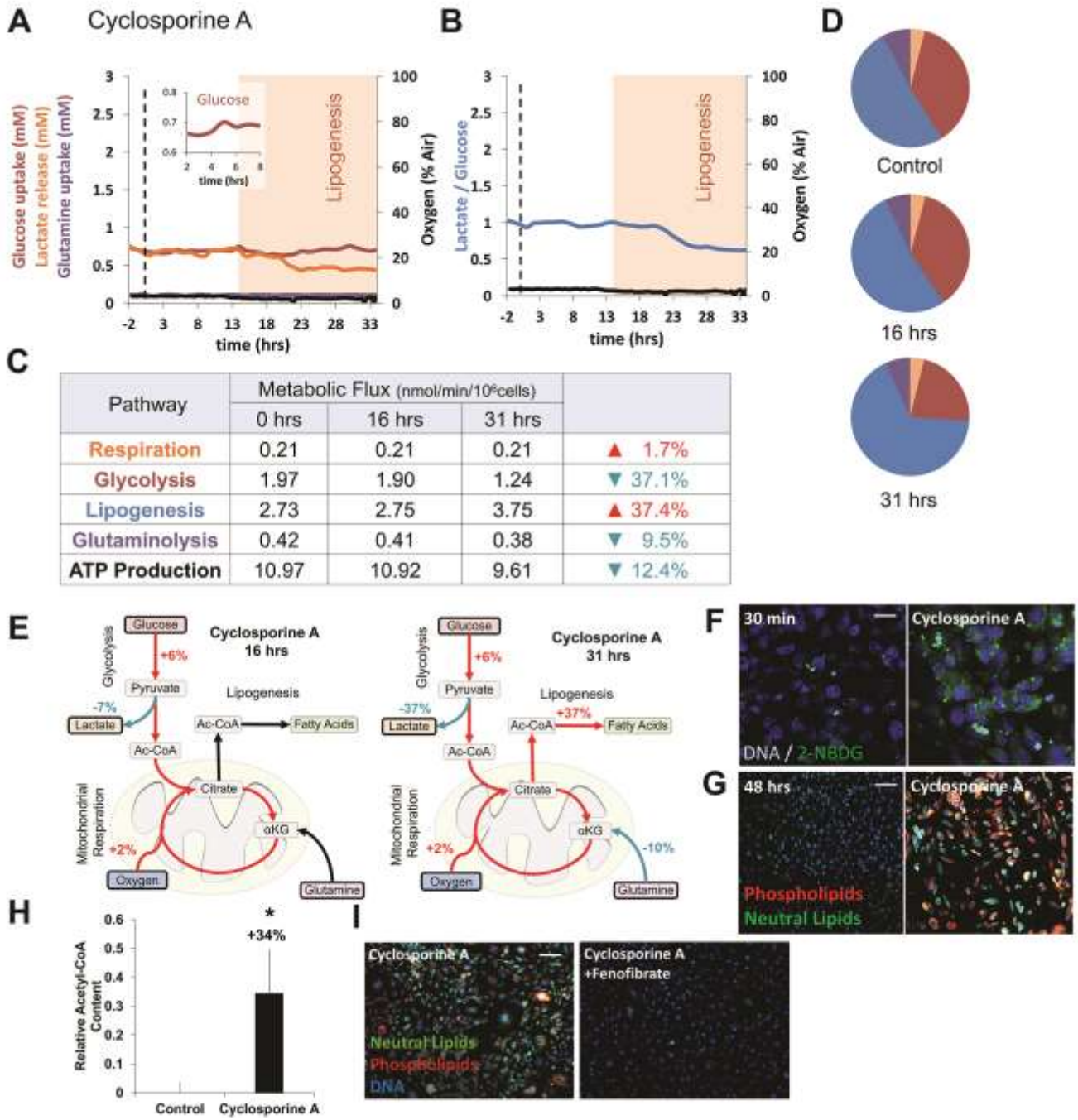

Pathway	Metabolic Flux (nmol/min/10⁶cells)			
	0 hrs	16 hrs	31 hrs	
Respiration	0.21	0.21	0.21	▲ 1.7%
Glycolysis	1.97	1.90	1.24	▼ 37.1%
Lipogenesis	2.73	2.75	3.75	▲ 37.4%
Glutaminolysis	0.42	0.41	0.38	▼ 9.5%
ATP Production	10.97	10.92	9.61	▼ 12.4%

Fig. S3. CsA induces a shift to lipogenesis. (A) Dynamics of oxygen, glucose, lactate and glutamine fluxes during continuous exposure of vascularized kidney organoids to physiological dose of cyclosporine under flow (1 μM). Glucose uptake increases by 6% within 2-3 hours of exposure (*insert*), lactate production drops following 13 hours of exposure. **(B)** Dynamics of lactate over glucose ratio following exposure to cyclosporine. Ratio drops by 30% after 13 to 20 hours of exposure, suggesting a shift in glucose utilization. **(C)** Intracellular metabolic fluxes calculated following 0, 16, and 31 hours exposure to sub-toxic concentration cyclosporine (>95% viability). Glucose utilization in each pathway is shown as nmol/min/10^6 cells as well as calculated ATP production. Lipogenesis increases by 37% while glycolysis and ATP production drop by 37% and 12%, respectively. **(D)** Relative glucose utilization is shown as a pie chart. Colors correspond to (A-C). Lipogenesis utilizes an increasing percentage of available glucose during cyclosporine exposure. **(E)** Flux balance analysis shows up-regulation of lipogenesis in kidney organoids exposed to cyclosporin for 31 hours. Red and

blue arrows note up- and down-regulated fluxes, respectively. **(F)** Glucose uptake assay in proximal tubule cells in monolayers within 30 min of cyclosporine exposure. 2-NBDG (green) is a glucose analog that is retained and accumulates in the cells suggesting that the loss of functional polarity disrupts the shuttling of the glucose transporter. **(G)** Fluorescence micrographs of neutral lipid (green) and phospholipidosis (red) in monolayers after 48 hours of cyclosporine exposure. **(H)** Quantification of acetyl-CoA detection assay in hPTC monolayers after 48 hours induction of 100 nM cisplatin. **(I)** Fluorescence micrographs of neutral lipid (green) and phospholipidosis (red) in monolayers after 48 hours of cyclosporine exposure, alone and in combination with 20 μM fenofibrate, a PPARα agonist. Scale bars = 10 μm. Student's *t*-test. *P < 0.05. n=3. N=3. Error bars indicate ± S.E.

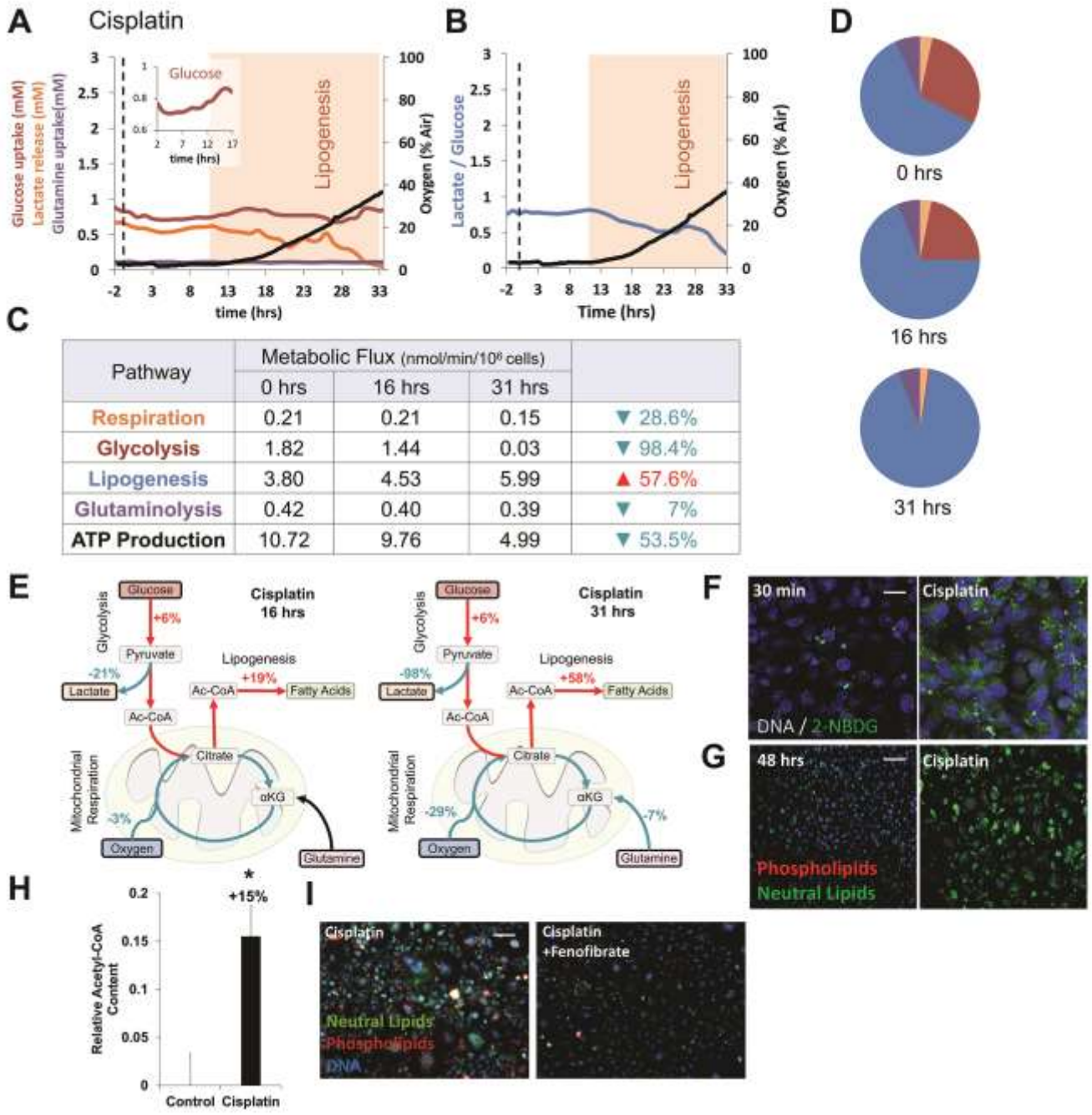

Pathway	Metabolic Flux (nmol/min/10^6 cells)			
	0 hrs	16 hrs	31 hrs	
Respiration	0.21	0.21	0.15	▼ 28.6%
Glycolysis	1.82	1.44	0.03	▼ 98.4%
Lipogenesis	3.80	4.53	5.99	▲ 57.6%
Glutaminolysis	0.42	0.40	0.39	▼ 7%
ATP Production	10.72	9.76	4.99	▼ 53.5%

Fig. S4. Cisplatin induces a shift to lipogenesis. (A) Dynamics of oxygen, glucose, lactate and glutamine fluxes during continuous exposure of vascularized kidney organoids to physiological dose of cisplatin (1 μM) under flow. Glucose uptake increases by 6% within 2-3 hours of exposure (*insert*), lactate production drops following 11 hours of exposure. **(B)** Dynamics of lactate over glucose ratio following exposure to cisplatin. Ratio drops by 55% after 11 hours exposure, suggesting a shift in glucose utilization. Intracellular metabolic fluxes calculated following 0, 16, and 31 hours exposure to sub-toxic concentration cisplatin. Glucose utilization in each pathway is shown as nmol/min/10^6 cells as well as calculated ATP production. Lipogenesis increases by 58% while glycolysis and ATP production drop by 98% and 53%, respectively. **(D)** Relative glucose utilization is shown as a pie chart. Lipogenesis utilizes an increasing percentage of available glucose during cisplatin exposure. **(E)** Flux balance analysis shows up-regulation of lipogenesis in kidney organoids exposed to cisplatin for 16 hours. Red and green arrows note up- and down-regulated fluxes, respectively. **(F)** Glucose uptake

assay in proximal tubule cells in monolayers within 30 min of cisplatin exposure. 2-NBDG (green) is a glucose analog that is retained and accumulates in the cells suggesting that the loss of functional polarity disrupts the shuttling of the glucose transporter. **(G)** Fluorescence micrographs of neutral lipid (green) and phospholipidosis (red) in monolayers after 48 hours of cisplatin exposure. **(H)** Quantification of acetyl-CoA detection assay in hPTC monolayers after 48 hours induction of 100 nM Cyclosporine A. **(I)** Fluorescence micrographs of neutral lipid (green) and phospholipidosis (red) in monolayers after 48 hours of cisplatin exposure, alone and in combination with 20 µM Fenofibrate. Scale bars = 10 µm. Student's *t*-test. *P < 0.05. n=3. N=3. Error bars indicate ± S.E.

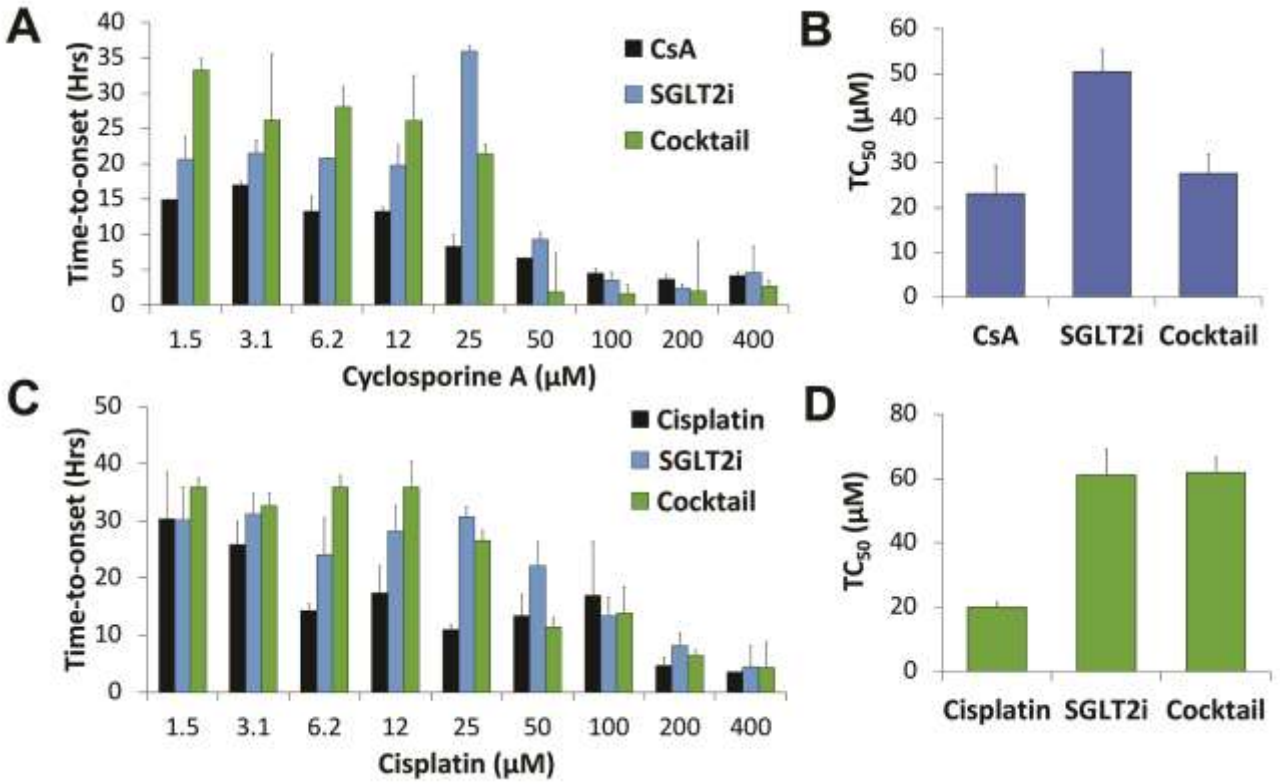

Fig. S5. Glucose inhibition shifts the onset of cellular damage. (A) Quantification of time-to-onset of damage in kidney spheroids of increasing concentrations of cyclosporin, cyclosporin and 5 µM empagliflozin (SGLT2i), or a cocktail of cyclosporin, 5 µM empagliflozin and 1 mM phloretin (Cocktail). **(B)** Quantification TC_{50} values following 48 hours of drug exposure. **(C)** Quantification of time-to-onset of damage in kidney spheroids of increasing concentrations of cisplatin, cisplatin and 5 µM empagliflozin (SGLT2i), or a cocktail of cisplatin, 5 µM empagliflozin and 1 mM phloretin (Cocktail). **(D)** Quantification TC_{50} values following 48 hours of drug exposure. Error bars indicate ± S.E.

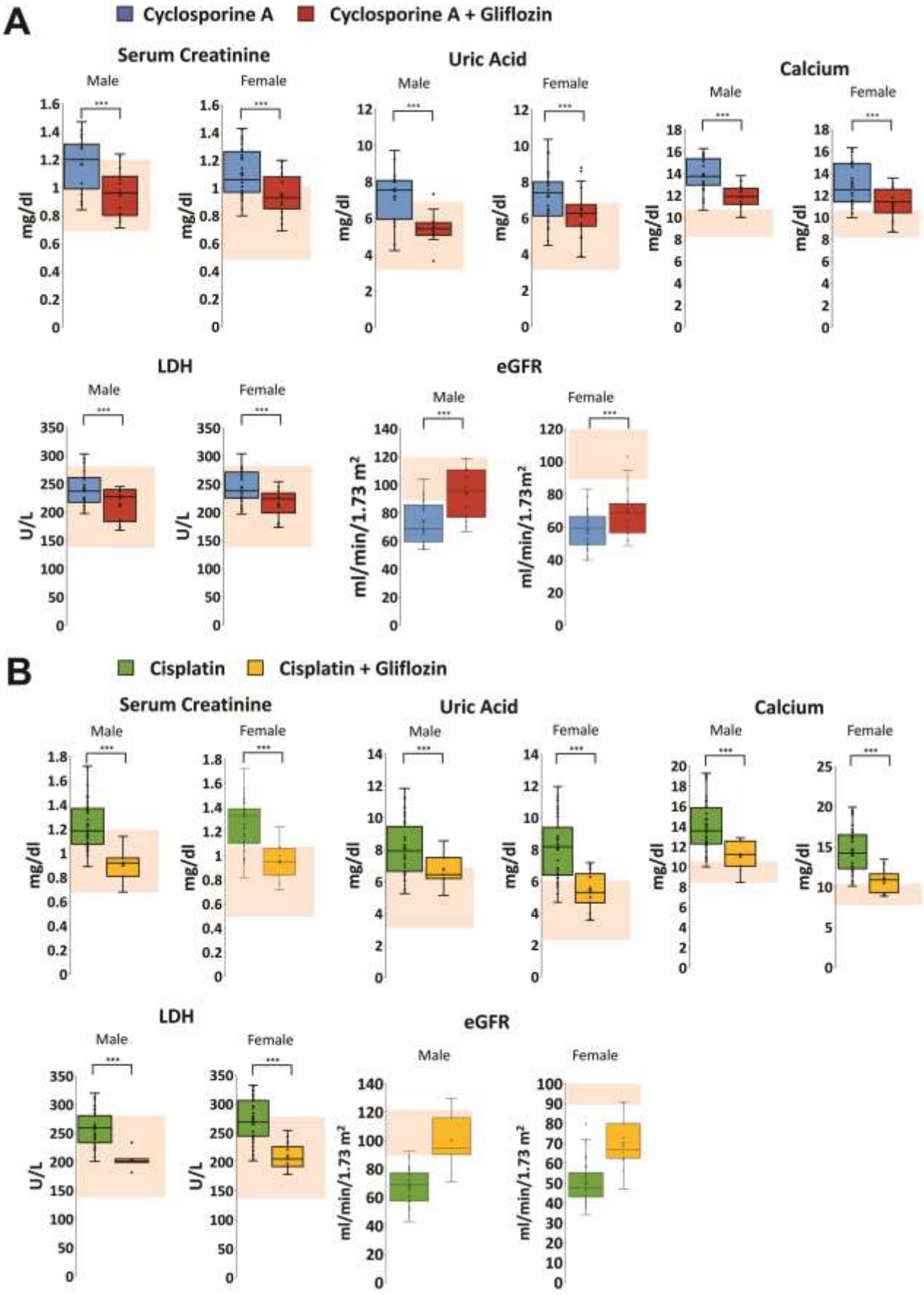
A
Cyclosporine A
Cyclosporine A + Gliflozin
Serum Creatinine
Male
Female
mg/dl
Uric Acid
Male
Female
mg/dl
Calcium
Male
Female
mg/dl
LDH
Male
Female
U/L
eGFR
Male
Female
ml/min/1.73 m²
B
Cisplatin
Cisplatin + Gliflozin
Serum Creatinine
Male
Female
mg/dl
Uric Acid
Male
Female
mg/dl
Calcium
Male
Female
mg/dl
LDH
Male
Female
U/L
eGFR
Male
Female
ml/min/1.73 m²

Fig. S6. Clinical validation in human patients segmented by sex. (A) Box plots showing serum creatinine, uric acid, calcium levels, lactate dehydrogenase (LDH), and estimated glomerular filtration rate (eGFR) in male and female patients treated with cyclosporin compared to those treated with both cyclosporin and empagliflozin (gliflozin). Shaded area indicates normal values varying by patient sex. **(B)** Box plots showing serum creatinine, uric acid, calcium levels, lactate dehydrogenase (LDH), and estimated glomerular filtration rate (eGFR) in male and female patients treated with cisplatin compared to those treated with both cisplatin and empagliflozin (gliflozin). Shaded area indicates normal values varying by patient sex. Error bars indicate ± S.E. Box plot center line indicate median, the cross indicate mean, box upper and lower limits indicate third and first quartiles respectively, whiskers 1.5x interquartile range, points are data points. Student's *t*-test. ***$P < 0.001$.

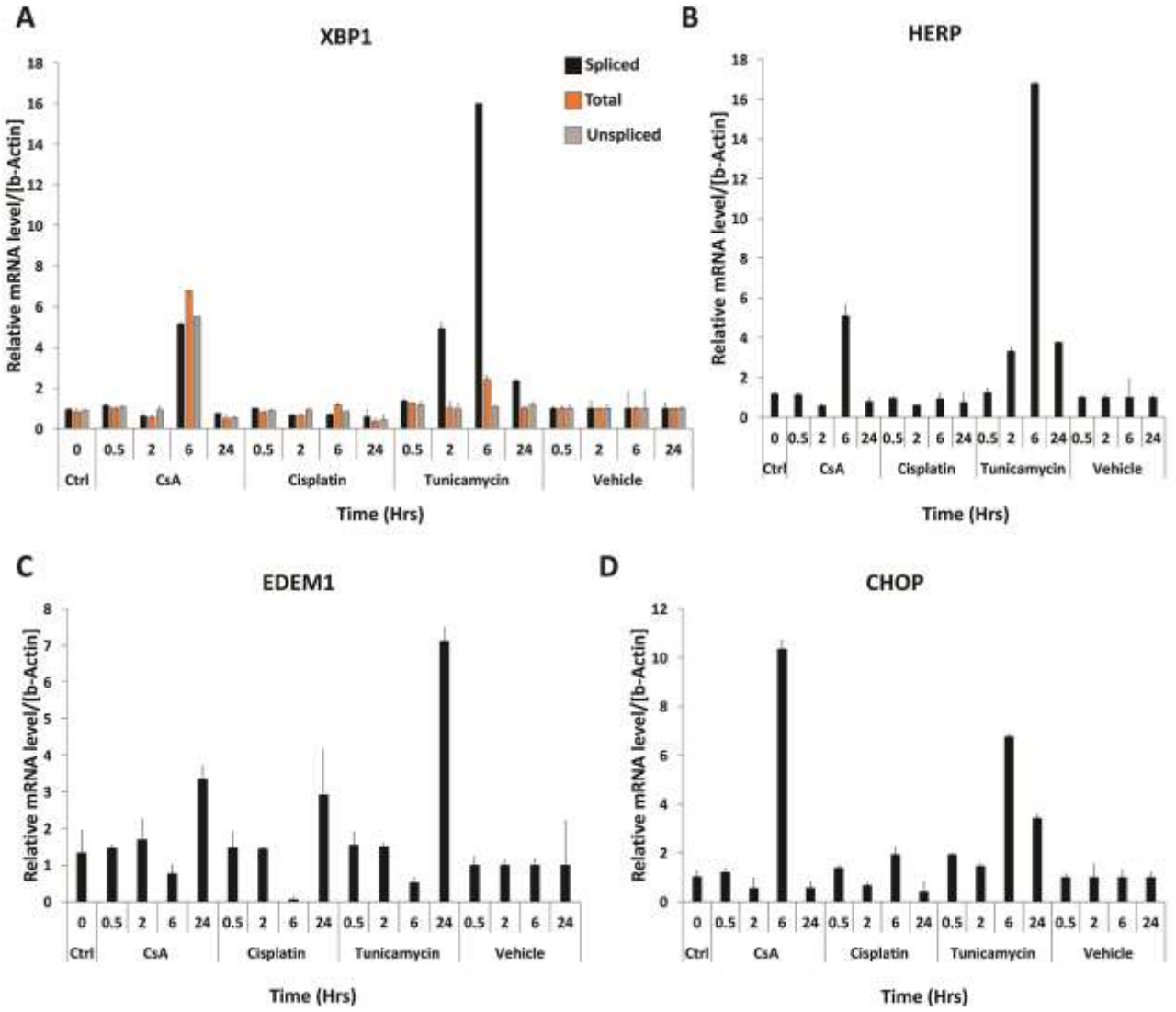

Fig. S7. Expression of endoplasmic reticulum stress markers after drug exposure. Relative mRNA of XBP-1 spliced (active form), XBP-1 unspliced (non-active form) and XBP-1 Total **(A)**, HERP (or HERPUD1) **(B)**, EDEM1 **(C)** and CHOP (or DDIT3) **(D)** normalized over B-Actin in hPTC monolayers after exposure of 1 nM of cyclosporine A (CsA) and 1 μM of cisplatin for 0, 0.5, 2, 6 and 24 hours. Controls were not exposed to any drugs; tunicamycin 5 μg/ml served as positive control and

the vehicle (0.025% DMSO) served as negative control. All conditions were composed of 3 biological replicates. Error bars: ± SE.

Table S1. Expression analysis of vascularized kidney spheroids. Enrichment analysis of mature human proximal tubule tissue monolayers compared with (**A**) vascularized spheroids and (**B**) in vivo proximal tubules.

A *Enrichment Analysis: hPTC Monolayer vs. Vascularized Spheroid*

Enriched Pathway	Count	%	P-Value	Benjamini	Category
Metabolic pathways	32	9.8	3.00E-08	5.80E-06	KEGG
Focal adhesion	18	5.5	1.20E-04	3.70E-03	KEGG
Gap junction	10	3.1	1.30E-03	1.40E-02	KEGG
Mineral absorption	8	2.4	1.00E-03	1.20E-02	KEGG
Regulation of sodium reabsorption	8	2.4	7.40E-04	9.70E-03	KEGG
Response to progesterone	8	2.4	2.70E-03	9.40E-02	Go BP
Gluconeogenesis	8	2.4	3.70E-03	9.20E-02	Go BP
Regulation of renal sodium excretion	8	2.4	9.60E-03	9.40E-02	Go BP
Hyperosmotic response	4	1.2	9.60E-03	9.40E-02	Go BP

327 differentially expressed genes (P < 0.001, q < 0.01), 31,036 background genes

B *Enrichment Analysis: hPTC Monolayer vs. In Vivo Proximal Tubule*

Enriched Pathway	Count	%	P-Value	Benjamini	Category
Metabolic pathways	58	17.7	5.80E-09	1.08E-06	KEGG
Focal adhesion	33	10.1	2.43E-05	7.21E-04	KEGG
Gap junction	21	6.4	2.60E-04	2.78E-03	KEGG
Mineral absorption	17	5.2	1.94E-04	2.41E-03	KEGG
Regulation of sodium reabsorption	15	4.6	1.26E-04	1.66E-03	KEGG
Response to progesterone	16	4.9	1.84E-04	1.76E-02	Go BP
Gluconeogenesis	14	4.3	5.39E-04	1.93E-02	Go BP
Regulation of renal sodium excretion	15	4.6	7.01E-04	1.75E-02	Go BP
Hyperosmotic response	8	2.4	2.00E-03	1.91E-02	Go BP

513 differentially expressed genes (P < 0.001, q < 0.01), 30,850 background genes

Table S2. List of qRT-PCR primers.

Gene	Forward Primer	Reverse Primer
FASN	5’- TTCTACGGCTCCACGCTCTTCC-3’	5’- GAAGAGTCTTCGTCAGCCAGGA-3’
SREBP1c	5’-GCTGTCCACAAAAGCAAATCT-3’	5’-GTCAGTGTGTCCTCCACCTCA-3’
HMGCR	5’-GATGGGAGGCCACAAAGAG-3’	5’-TTCGGTGGCCTCTAGTGAGA-3’
UCP2	5’-GAACGGGACACCTTTAGAGAAG-3’	5’-CCGTGAGACCTTACAAAGCC-3’
CPT2	5’-GCAGATGATGGTTGAGTGCTCC-3’	5’- AGATGCCGCAGAGCAAACAAGTG-3’
COX2	5’-TAGACAGCGTAAACTGCGCCT-3’	5’-TGCCCCACAGCAAACCGTAG-3’
b-Actin	5’-ATCATGTTTGAGACCTTCAAC-3’	5’-CATCTCTTGCTCGAAGTCCA-3’
RPL32	5’- ACAAAGCACATGCTGCCCAGTG-3’	5’- TTCCACGATGGCTTTGCGGTTC-3’
XBP1 Spliced	5’-ACGAGAGAAAACTCATGGCCT-3’	5’-TGCACCTGCTGCGGAC-3’
XBP1 Unspliced	5’-AGAGAAAACTCATGGCCTTGTAGT-3’	5’-GAGGTGCACGTAGTCTGAGT-3’
XBP1 Total	5’-CCCTTTCCCCATTCAGTGACA-3’	5’-CCTCCAGGCAGTGTAATAGTCA-3’
EDEM1	5’-GGCCCCCGCGCTTTAAAATA-3’	5’- GGAAAGCGCTGGTAGAAGCC-3’
CHOP	5’- AAGTCTAAGGCACTGAGCGT-3’	5’- GCTGGTCTGATGCCTGCTTTC-3’
HERP	5’- CTATGAATGACCCTGGCAGAGAC-3’	5’- TCTTACCGGCACAAACAGTCC-3’

Table S3. List of antibodies and probes.

Antibodies and probes	Species	Cat. Number	Concentration
Anti-AQP1	Rabbit	Abcam ab168387	1:100
Anti-TIM-1/KIM-1/HAVCAR	Mouse	R&D Systems AF1750	1:100
Fluorescein labeled LTL		Vector Laboratories FL-1321	1:50
Rhodamine Phalloidin		Invitrogen R415	1:20
Hoechst 33258		Sigma B2883	1:1000
Anti-Mouse Alexa Fluor 647	Donkey	Abcam ab150107	1:100
Anti-Rabbit Alexa Fluor 488	Donkey	Abcam ab150073	1:100

Other files (Excel format):
Data file S1. Raw data.

Movie S1. 3D reconstruction from LSM700 confocal Z-stack of a vascularized kidney spheroid labeled with AQP1. 360 degrees X-rotation emphasizes parallel longitudinal tubular structures.